

Nanostructure Modification of Welds Metal HSLA Steels by Oxide Particles

Valery Kostin^{1*}, Viktor Golovko², Viktor Zhukov¹, Olga Kushnarova¹, Maksim Reminnyi³, and Aleksandr Puzrin¹

¹Department Materials Science, E.O. Paton Electric Welding Institute Kyiv, Ukraine

²Department Welding HSLA Steels, E.O. Paton Electric Welding Institute Kyiv, Ukraine

³Department of Applied Physics and Materials Science, Kyiv Academic University, Kyiv, Ukraine

*Corresponding author:

Valery Kostin, Department Materials Science, E.O. Paton Electric Welding Institute Kyiv, Ukraine.

ABSTRACT

In the article was presented investigation performed on the nano-sized particles of refractory oxides Al_2O_3 , TiO_2 , MgO , ZrO_2 inoculation into the welding pool. It is shown that the oxides inoculation with a low level of mismatch to the δ -Fe lattice and increased wetting with liquid iron (MgO , ZrO_2) into the weld pool contributes to the dendrite's growth, which are formed during melt crystallization. Metal modification with MgO , ZrO_2 oxides contributes to a decrease the polygonal ferrite hardness and an increase in the lower bainite content in the microstructure, increasing the metal resistance against brittle fracture. Metal modification with oxides Al_2O_3 , TiO_2 contributes to an increase of polygonal ferrite hardness and increase of the upper bainite content in the microstructure, and growth strength indicators of low-alloy steel welds.

Keywords: Low-alloy Steel, Welding, Microstructure, Modification, Inoculation, Nanosized Oxides.

Received: April 17, 2025;

Accepted: April 23, 2025;

Published: April 30, 2025

Introduction

Despite the rapid development and wide use of various composite and polymer materials in recent times, steel still remains the main material in the welded metal structures manufacture in various economy branches. The most noticeable growth rates are characteristic of high-strength, low-alloy steels. The expansion of objects in which HSLA steel is used is accompanied by their production technology improvement [1, 2]. Due to the fact that the high-strength steels structures manufacture, repair and restoration are associated with the wide use of welding processes, the problem of the welded joint's reliability increasing in accordance with the mechanical properties base metal level is highly relevant.

The HSLA steels expansion use is associated with a strength, plasticity and viscosity indicators effective combination, which are achieved as a complex manufacturing processes result [3]. Welding processes have a significantly smaller technological approaches list to solving the problem of ensuring a welded joints mechanical properties complex. The entire steel welding technological process is based

on understanding the mechanisms of the metal structure formation and the structure parameters control (size of grains, phases, inclusions) weld metals. The more control is given over this process; the higher weld metals mechanical properties level can be obtained. One of the common methods for increasing the weld metal viscosity without reducing their strength is the weld metal modification process (Figure 1).

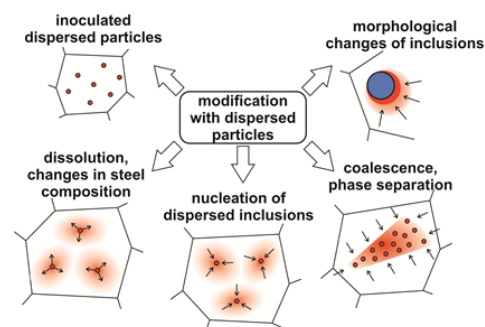


Figure 1: Mechanisms of welding metal modification with dispersed particles.

The metal modification process has long been used both in the steel castings production and in welding in order to influence the metal mechanical properties set. Recently, publications

Citation: Valery Kostin, Viktor Golovko, Viktor Zhukov, Olga Kushnarova, Maksim Reminnyi, et al. (2025) Nanostructure Modification of Welds Metal HSLA Steels by Oxide Particles. J Modr Sci Scient Res 1: 1-5.

have appeared in the scientific and technical literature, which show the expediency of inoculating refractory compounds nanosized particles into the metal melt to modify the metal in the crystallization process and microstructure formation [4-6]. Works have been carried out in which the nanoscale inoculants influence on the welds metal properties has been shown [7, 8].

One of the effective mechanisms for modifying the structure is associated with an increase in the metal melt crystallization centers.

Materials and Research Method

Objectives

This work purpose was to investigate the nanosized refractory inoculants effect on the HSLA welds metal microstructure formation.

Materials and Conditions for Obtaining of Welded Joints

In order to study the effect of nanoparticles on the formation of the structure and mechanical properties of the weld metal, butt-welded joints of sheets of HSLA S355J2 steel type (0.18% C, 0.33% Si, 0.98% Mn, <0.025% P, < 0.025% S, 0.45% Cu) with a yield strength up to 650 MPa were made. Welds metal was performed according to the method during arc welding in a shielding gas environment (82% Ar, 18% CO₂) with a "metalcore" type flux-cored wire (a diameter of 1.6 mm) at a of 200 (±5) A direct current, 30 (±2) V arc voltage with of 21 (±2) kJ/cm an input energy [8]. The energy level at the non-metallic inclusion boundary with a metallic phase can be estimated through the wetting angle. Therefore, refractory compounds with different levels of wetting by the metal phase were chosen as inoculants Table 1. The results of determining the mechanical properties are shown in Table 2.

For determination the non-metallic inclusions influence nature on the weld metal microstructure formation, a powder wire with a 1.6 mm diameter was introduced into the "cold" part of the welding bath. The introduced wire core contained a particles mixture (10% of refractory compounds with a size of 0.040...0.200 mm and 90% of iron powder according to DSTU 9849). The general view of the initial refractory particles is shown in Figure 2. The obtained results were compared with the data of weld metal obtained with welding without introduced flux-cored wire (weld metal HH-0).

Techniques and Equipment for Research

The chemical composition of the weld metal was determined using an inductively coupled plasma emission spectrometer of the iCAP 6500 DUO (Thermo Fisher Scientific, USA), which has impressive detection limits and analysis speed.

Metallographic studies were carried out on cross sections cut from welded joints. The welds metal structure was studied using a Neophot 32 optical microscope. Microstructure detection in the samples was carried out by the chemical etching method in a 4% alcoholic solution of nitric acid (nital). Samples for research were made according to standard methods using different dispersion diamond pastes. The structural components size was.

determined in accordance with DSTU 8972-2019

The microhardness of the structural components was measured on the LECO company M-400 hardness tester at loads of 100 g (HV0.1) and 1 kg (HV10) according to DSTU 2999.

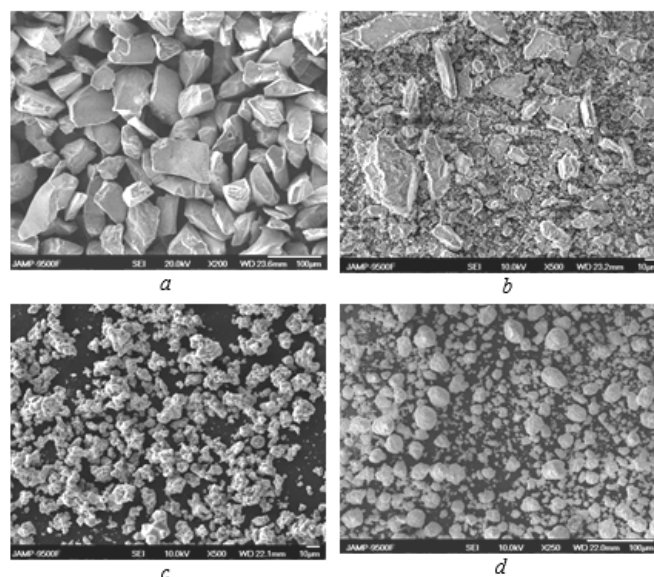


Figure 2: Appearance of modifier inoculant powders: a-Al₂O₃; b - MgO; c - TiO₂; d-ZrO₂

The welds metal mechanical properties were determined in accordance with the standards DSTU ISO 6892-1:2019 and DSTU EN 10045-1:2006, as well as DSTU ISO 5792-1-2009 for testing at low temperatures. The structural transformations nature in the welds metal was studied by the thermal welding deformation cycle simulating method using the Gleeble 3800 complex equipped with a high-speed dilatometer. The research was carried out using cylindrical samples with 6.0 mm diameter and 80 mm length, made from welds metal. According to the developed in the E. O. Paton EWI method, the samples were heated in a vacuum chamber to a temperature of 1170 °C according to a given program, and then cooled according to various thermal cycles. The cooling curves corresponded to the Newton-Richmann dependence and corresponded to the cooling rates of metal 5; 10; 17; 30; 45 °C/s in the temperature range of 500-600 °C.

Table 1: Welds Metal Chemical Composition

| №№ weld | Хімічний склад, мас. % | | | | | | | | | | Inoculant |
|---------|------------------------|------|------|-------|-------|------|------|------|-------|-------|--------------------------------|
| | C | Si | Mn | S | P | Cr | Ni | Mo | Al | Ti | |
| HH-0 | 0,042 | 0,34 | 1,19 | 0,021 | 0,020 | 0,10 | 2,13 | 0,28 | 0,028 | 0,029 | - |
| HH-22 | 0,035 | 0,40 | 1,24 | 0,016 | 0,021 | 0,11 | 1,97 | 0,27 | 0,031 | 0,017 | TiO ₂ |
| HH-23 | 0,034 | 0,42 | 1,40 | 0,017 | 0,023 | 0,15 | 2,15 | 0,29 | 0,032 | 0,015 | Al ₂ O ₃ |
| HH-24 | 0,031 | 0,22 | 1,11 | 0,025 | 0,024 | 0,14 | 1,85 | 0,29 | 0,023 | 0,030 | MgO |
| HH-25 | 0,033 | 0,22 | 1,05 | 0,024 | 0,024 | 0,12 | 2,02 | 0,30 | 0,024 | 0,031 | ZrO ₂ |

Table 1: Welds Metal Chemical Composition

| №№ weld | Rm | Re | A | Z | KCV, J/cm ² at T, °C | | | | Inoculant |
|---------|-------|-------|------|------|---------------------------------|------|------|------|--------------------------------|
| | MPa | | % | | + 20 | 0 | - 20 | - 40 | |
| HH-0 | 693 | 605 | 14,5 | 48,4 | 97 | 87 | 75 | 53 | - |
| HH-22 | 708,7 | 636,4 | 19,3 | 56,7 | 84,6 | 71,7 | 60,0 | 50,0 | TiO ₂ |
| HH-23 | 728,2 | 621,4 | 17,5 | 54,4 | 82,1 | 58,3 | 50,4 | 35,8 | Al ₂ O ₃ |
| HH-24 | 644,5 | 586 | 18,6 | 59,9 | 102,9 | - | 69,2 | 60,0 | MgO |
| HH-25 | 621,6 | 532,2 | 19,5 | 65 | 119,6 | - | 72,9 | 64,6 | ZrO ₂ |

At the same time, the cooling parameters of thermal welding cycles (thermal and time) in the welds metal during welding were quite accurately reproduced. When studying the austenite decay kinetics, the beginning and end temperatures of the transformation were determined according to the method presented in [9]

The microstructure dispersion level was studied by scanning electron microscopy (SEM) on a JSM-840 microscope (JEOL, Japan) in the secondary electron (SEI) mode at an accelerating voltage of 20 kV and a probe current of 10-7A. The electron microscope is equipped with a combined energy dispersive microanalysis system INCA PentaFet x3 ("INCA", Great Britain). The state of grain the primary austenite structure is the basis of the welds secondary structure formation processes, which corresponds to the entire its mechanical properties complex. The austenite microscopy (TEM) using a JEM-200-CX microscope (JEOL, Japan).

Results and Discussion

The welds metal chemical composition is given in Table 1. The results of determining the mechanical proper-ties are shown in Table 2. The wetting angle of oxides that were used as inoculants for the welding pool are shown in Figure 3 [10]. Physicochemical characteristics of the powders that were used as inoculants are given in Table 3.

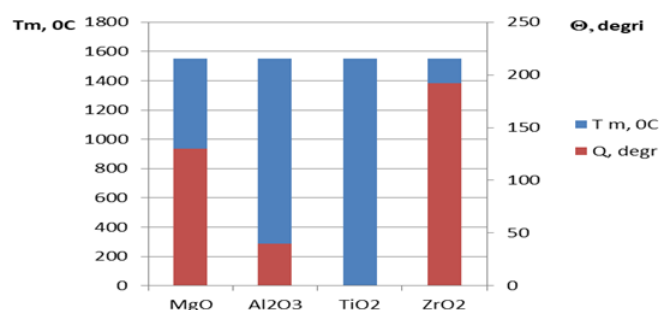


Figure 3: Temperature of melting (T_m) and wetting angle at the oxide/iron interface (θ) [10]

The microstructure of the investigated welds metal, which were modified with various metals refractory oxides (TiO₂, Al₂O₃, MgO, ZrO₂), was investigated by the optical metallography methods Figure 4. Quantitative metallography method was used to determine the dendrites and the primary structure grains sizes (Figure 5a), hardness (AF and PF) (Figure 5b) and the proportion of structural components in the welds metal (Table 4).

The primary austenite structure is the basis of the welds secondary structure formation processes, which corresponds to the entire its mechanical properties complex. The austenite transformation occurs in the high temperature range Ac₃–Ac₁, which depends on the weld metal cooling rate. To check this temperature rang effect on the dendritic structure formation, dilatometric studies were conducted.

Table 3: Physical-chemical Characteristics of Compounds Used as Inoculants[10]

| Inoculant | T _{melt} , °C | Crystal lattice type | Lattice parameter, nm | Size mismatch δ -Fe, % | Inter-phase energy, mJ/m ² |
|--------------------------------|------------------------|----------------------|-----------------------|------------------------|---------------------------------------|
| ZrO ₂ | 2715 | Tetragonal | a-3,640 c-5,152 | 1 | 2863 |
| MgO | 2825 | Face-centered cubic | a-4,213 | 14 | 2226 |
| TiO ₂ | 1843 | Tetragonal | a-4,593 c-2,959 | 25 | 2444 |
| Al ₂ O ₃ | 2044 | Rhombohedral | a-5,120 α-55,25° | 39 | 972 |

During the dilatometric analysis, the thermal regimes corresponding to the cooling rates in the temperature range of 800...500 °C were selected - 5, 10, 17, 30 and 45 °C/s. The tests were carried out on the Gleeble 3800 unit, which made it possible to accurately repeat the welding thermal cycle on each weld metal studied composition. As a result of comparison, the real welds metal structural components proportion with the welds metal dilatometric tests, it was determined that the welds metal cooling rate was in the range of 12 - 17 °C/s.

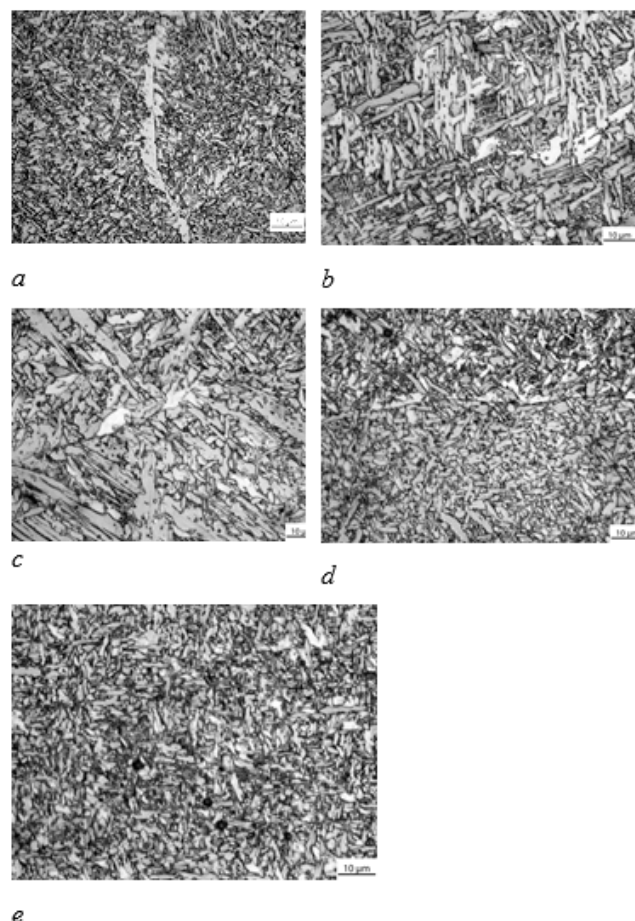


Figure 4: Microstructure of metal samples of seams modified with inoculants: a- without inoculants; b - TiO₂; c - Al₂O₃; d - MgO; e - ZrO₂

Table 4: Share (%) of Microstructural Components of Metal of Welds

| Inoculant | Ferrite | | | | | Bainite | | Others |
|--------------------------------|---------|----|----|----|----|---------|-------|--------|
| | AF | PF | IZ | GF | WF | Upper | Lower | |
| – | 8 | 5 | 8 | 2 | 15 | 40 | 17 | 5 |
| TiO ₂ | 5 | 5 | 0 | 0 | 32 | 43 | 10 | 5 |
| Al ₂ O ₃ | 2 | 2 | 0 | 0 | 30 | 48 | 11 | 7 |
| MgO | 32 | 10 | 0 | 10 | 7 | 15 | 21 | 5 |
| ZrO ₂ | 30 | 15 | 2 | 6 | 7 | 10 | 25 | 5 |

Notes: AF - acicular ferrite; PF - polygonal ferrite; IZ - intra-granular ferrite; GF - globular ferrite; WF - Widmannstätt ferrite.

Thermokinetic diagrams of austenite transformation for different types of inoculants were constructed (Fig.6). The data of dilatometric studies, as well as the volume fraction transformation data dependence on the temperature, indicate a

monotonous course phase transformation, when it is not possible to distinguish the points of intermediate phases occurrence, except for the beginning and end transformation points, for all cooling rates.

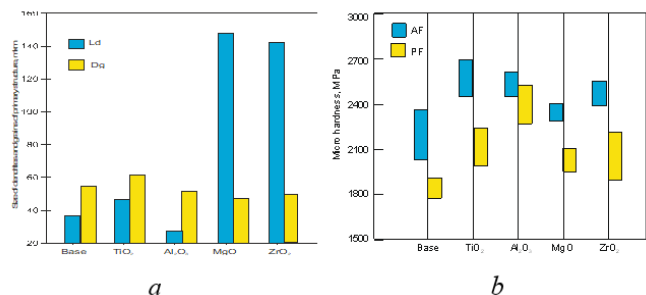


Figure 5: Properties of metal modified welds metal: a - size of the dendrites (Ld) and the primary structure grains (Dg); b - microhardness (HV0,1).

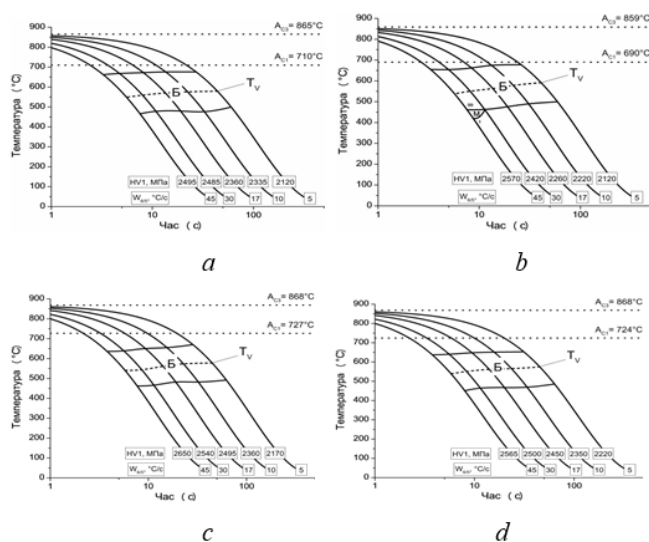


Figure 6: Thermokinetic diagrams transformation of austenite in the metal of modified welds: a - without modification; modification with: b - ZrO₂; c - TiO₂; d - Al₂O₃

In addition to the primary austenite grains morphology, the weld metal secondary structure formation is influenced by the bainite transformation beginning and end temperature. The bainite formation kinetics was evaluated by the B50 index, which corresponds to the bainite phase 50% formation temperature.

In order to identify the factors that influence these processes, a comparative of the welds metal dilatograms analysis was performed, the results of which are shown in Figure 7.

The results of dilatometric studies (Figure 6, 7) showed that the inoculations in the welding pools with aluminum and titanium oxides reduces the austenite decomposition temperature range by increasing its completion temperature. Modification with magnesium and zirconium oxides contributes to the more massive dendrites formation during metal crystallization (Figure 5a). When magnesium and zirconium oxides nanoparticles are introduced into the welding pool melt, the bainitic beginning and end transformation temperature increases significantly (Figure 7).

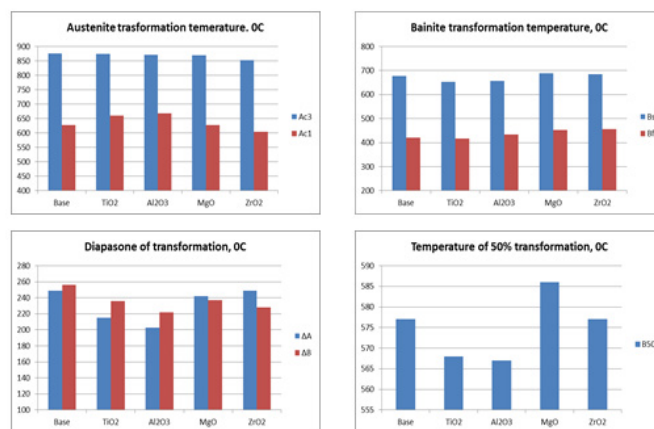


Figure 7: Parameters of austenite decomposition diagrams in the welds metal structure. Notes: Ac3 - the of the austenite formation beginning; Ac1 - the austenite breakdown beginning; ΔA is the austenite decay range; Bs is the bainite transformation beginning; Bf - bainite transformation end; ΔB -bainite transformation range; B50 - is the temperature of 50% bainite formation.

An increase in the dendrites size and a decrease in the Bf temperature affects the carbon diffusion reduction from the austenite grains in the $\gamma \rightarrow \alpha$ transformation process, which contributes to the of an increased cementite content formation in the body and a decrease in their allocation at the ferrite grains boundaries. The probability of such a metallurgical reactions development is confirmed by the increased lower bainite content in the weld metal structure (Table 4) and the reduced the polygonal ferrite hardness level compared to the welds metal modified with aluminum and titanium oxides (Figure 5b).

The weld metal modification with aluminum and titanium oxides is accompanied by a decrease in the temperature at which the bainite transformation ends (Figure 6). As a result, the carbon amount that diffuses to the grain boundaries increases, the polygonal ferrite hardness level increases (Figure 4b) and the upper bainite content increases (Table 4).

Changes in the metal microstructure composition correspond to the determining their mechanical properties results. An increase in the polygonal ferrite hardness and the upper bainite content in the microstructure composition when modifying the weld metal with aluminum and titanium oxides is accompanied by an increase in strength indicators (Table 2). The welds metal modification with magnesium and zirconium oxides helps to increase the lower bainite content in the microstructure composition and increase the level of metal impact strength (Table 2).

From the data given in Table 3, it can be seen that the oxides inoculated into the welding pool differ in the inconsistency level of the crystal lattice parameters with iron and the wetting index by liquid iron (Figure 3). Magnesium and zirconium oxides, which are well wetted by molten iron, and whose crystal lattice size is close to the parameters of δ -Fe, should be nucleation centers of iron crystals at higher temperatures compared to the welds metal inoculated with aluminum and titanium oxides. This explains the difference in the dendrites size, which was established during the metallographic welds metal analysis (Figure 5a).

Reducing the refractory oxides size inoculated into the weld pool to nanosize (30...70 nm, Figure 7) which are comparable to the size of the tip of a growing dendrite in the steel melt increases the efficiency of the modification.

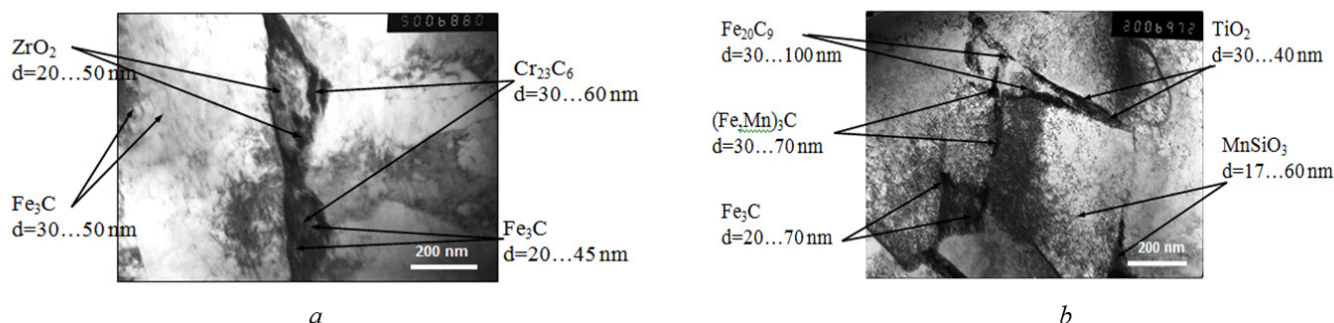


Figure 8: TEM image of oxide inoculants in weld metal: a - ZrO₂ (x50000); b - TiO₂ (x30000)

In order to expand the knowledge base regarding the features of low-alloy steels welds metal modification, studies on the refractory oxides Al₂O₃, TiO₂, MgO, ZrO₂ nano-sized particles inoculation into the welding pool were performed. The welds metal metallographic and dilatometric studies were conducted, and the results of determining their mechanical properties were obtained. As a carried-out investigations result, it was established:

1. Inoculation oxides into the weld pool with a low mismatch level to the δ -Fe lattice and increased wetting with liquid iron (MgO, ZrO₂) contributes to the dendrite's growth, which are formed during melt crystallization.
2. The welds metal modification with MgO, ZrO₂ oxides helps to reduce the polygonal ferrite hardness and increase the lower bainite content in the metal microstructure.
3. The welds metal modification with Al₂O₃, TiO₂ oxides increases the polygonal ferrite hardness and increases the upper bainite content in the metal microstructure.
4. As a result of metal modification with Al₂O₃, TiO₂ oxides, the low-alloy steel welds strength indicators increase, and modification with MgO, ZrO₂ oxides helps to increase the welds metal resistance against brittle fracture.

References

1. Varshney A, Sangal S, Kundu S, Monda K (2016) Super strong and highly ductile low alloy multiphase steels consisting of bainite, ferrite and retained austenite. *Materials and Design* 95: 75-88.
2. Lang V, Puerta J, Eriksson K, Francisca G Caballeroet, Carlos Garcia-Mateo, et al. (2013) New Advanced Ultra High Strength Bainitic Steels: Ductility and Formability (DUCTAFORM). Luxembourg: Publications Office of the European Union.
3. Halfa H (2014) Recent Trends in Producing Ultrafine Grained Steels. *Journal of Minerals and Materials. Characterization and Engineering* 2: 428-469.
4. Hsiung LL, Fluss MJ, Tumey SJ, Choi BW, Serruys Y, Kimura A (2010) Formation mechanism and the role of nanoparticles in Fe-Cr ODS steels developed for radiation tolerance. *Physical Review* 82: 184103-1 - 184103-13.
5. Schneibel JH, Kad BK (2007) Nanoprecipitates in steels. *Proceedings of the Twenty First Annual Conference on Fossil Energy Materials*, April 30-May 2.
6. Yu Stetsenko V (2015) Nanostructural processes of melting, crystallization and modification of metals. *Casting and metallurgy* 3: 51-53.
7. Kostin V, Berdnikova O, Zukov V, Grigorenko G (2020) Increase of Mechanical Properties of Weld Metal of High-Strength Low-Alloy Steels. *Microstructure and Properties of Micro- and Nanoscale Materials, Films, and Coatings (NAP 2019)*, A. Pogrebnjak and O. Bondar, Eds. Springer Proceedings in Physics 240.
8. Kostin VA, Grigorenko GM, Poznyakov VD, Zuber TO (2020) Structural Transformations of the Metal of Heat-Affected Zone of Welded Joints of High-Strength Armor Steels. *Materials Science* 55: 863-869.
9. Cherepin VT (1968) Experimental technique in physical metallurgy. Kyiv: Tekhnika 280.
10. Panasyuk AD, Fomenko VS, Glebova GG (1986) Resistance of non-metallic materials in melts. Kyiv: Naukova Dumka 352.